

GGA-Level Subsystem DFT Achieves Sub-kcal/mol Accuracy Intermolecular Interactions by Mimicking Nonlocal Functionals

Xuecheng Shao,* Wenhui Mi,* and Michele Pavanello*

Cite This: *J. Chem. Theory Comput.* 2021, 17, 3455–3461

Read Online

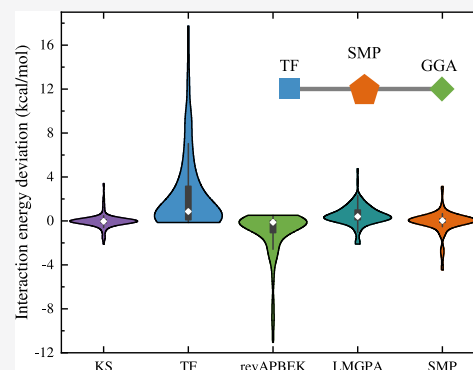
ACCESS |

Metrics & More

Article Recommendations

Supporting Information

ABSTRACT: The key feature of nonlocal kinetic energy functionals is their ability to reduce to the Thomas-Fermi functional in the regions of high density and to the von Weizsäcker functional in the region of low-density/high reduced density gradient. This behavior is crucial when these functionals are employed in subsystem DFT simulations to approximate the nonadditive kinetic energy. We propose a GGA nonadditive kinetic energy functional which mimics the good behavior of nonlocal functionals, retaining the computational complexity of typical semilocal functionals. Crucially, this functional depends on the inter-subsystem density overlap. The new functional reproduces Kohn–Sham DFT and benchmark CCSD(T) interaction energies of weakly interacting dimers in the S22-5 and S66 test sets with a mean absolute deviation well below 1 kcal/mol.



1. INTRODUCTION

Subsystem DFT (sDFT) is a divide-and-conquer method that extends the applicability of conventional DFT to system sizes larger than those typically accessible.^{1–4} The main idea behind sDFT is to split the noninteracting kinetic energy into subsystem additive and nonadditive parts.^{5–10} Namely

$$T_s[\rho] = \sum_I^{N_s} T_s[\rho_I] + T_s^{\text{nonadd}}[\{\rho_I\}] \quad (1)$$

where $\{\rho_I(\mathbf{r})\}$ is the set of subsystem electron densities. In doing so, orthogonalization of wavefunctions belonging to different subsystems is completely bypassed,¹¹ and a formally linear-scaling behavior can be attained (or quasi-linear due to the need to solve for Coulomb interactions which scales like $O(N \log(N))$).^{12–17} Naturally, for the method to be accurate, the additive terms are treated exactly (*i.e.*, the kinetic energy internal to the subsystems is evaluated with the subsystem orbitals), while to improve efficiency, the nonadditive functional is defined simply through eq 1 and is evaluated with pure density functionals. Clearly, the accuracy of the method is directly related to the quality of the pure functionals employed as nonadditive functionals.^{18–22}

The common strategy in sDFT is to borrow already available pure density functionals for the noninteracting kinetic energy and use them in eq 1 to obtain approximations for the nonadditive kinetic energy functional (NAKE). LDA, GGA, and nonlocal NAKes have been proposed by this strategy. GGA NAKes already provide a semiquantitative description of inter-subsystem interactions (molecule–molecule and molecule–surface).^{22–24} However, only recently nonlocal functionals (*i.e.*,

functionals that depend on the density evaluated simultaneously in two or more separate points in space) have been employed as a NAKE with great success.^{25–27} Such GGA nonadditive functionals as revAPBEK and LC94 are expected to perform with an accuracy averaging slightly above 1 kcal/mol; however, the shape of the energy curves are incorrectly too attractive (see refs 25, 24, and *vide infra*). When these functionals are corrected by a fitted repulsive function (in the same spirit as the repulsive part of a Grimme’s Dn correction), the shape of the energy curves involved is significantly improved.²⁴ Nonlocal functionals also make very good NAKes and further improve the performance of GGA NAKes in sDFT simulations to a mean absolute deviation (MAD) below 1 kcal/mol for the S22-5 set, with particularly strong improvement for strained structures and correctly reproducing the shape of the energy curves.²⁵

The question we address in this work is can we achieve an accuracy similar to the one of nonlocal functionals with a GGA functional? Since the early work on GGA NAKes,²⁸ it became clear that in order to satisfy the non-negativity condition, $T_s^{\text{nonadd}} \geq 0$, it is important to use the Thomas-Fermi functional, $T_{\text{TF}}[\rho] = \int \tau_{\text{TF}}(\rho(\mathbf{r})) d\mathbf{r} = \int \rho^{5/3}(\mathbf{r}) d\mathbf{r}$, for low values of the reduced gradient, $s(\mathbf{r}) = |\nabla\rho(\mathbf{r})|/(2\rho(\mathbf{r})k_F(\mathbf{r}))$, where $k_F(\mathbf{r}) = (3\pi^2\rho(\mathbf{r}))^{1/3}$ is the local Fermi wavevector. To easily achieve this, an enhancement factor, F_s , is introduced. Namely

Received: March 23, 2021

Published: May 13, 2021



$$T_s^{\text{GGA}}[\rho] = \int \tau_{\text{TF}}(\rho(\mathbf{r})) F_s(s(\mathbf{r})) d\mathbf{r} \quad (2)$$

Such a strategy is commonplace. It is found in, for example, the revAPBEK²⁹ kinetic energy functional and many others.^{28,30,31} They share the following approximate form of the enhancement factor borrowed from the PBE exchange functional³²

$$F_s^{\text{approx}}(s) = 1 + \frac{\kappa s^2}{1 + \frac{\kappa}{\mu} s^2} \quad (3)$$

Laricchia *et al.*²⁹ found that revAPBEK outperformed all other GGA functionals. Thus, in this work, we use revAPBEK as a reference for the performance of GGA functionals.

Nonlocal functionals achieve the goal of functional positivity by providing the following ansatz for the kinetic energy functional^{33,34}

$$T_s[\rho] = T_{\text{TF}}[\rho] + T_{\text{vW}}[\rho] + T_{\text{NL}}[\rho] \quad (4)$$

where T_{vW} is the von Weizsäcker kinetic energy (which violates positivity³⁵) and T_{NL} is the nonlocal contribution. T_{NL} is designed to cancel out T_{TF} in the tail of atoms where T_{vW} is expected to be accurate and to cancel out T_{vW} in the regions of the high-density/low-density gradient where T_{TF} is expected to be accurate. Thus, it is not a surprise that nonlocal nonadditive functionals are the currently best-performing NAKEs.²⁵

2. SMP FUNCTIONAL

Cognizant of the analysis above, we set out to develop a NAKE that takes inspiration from the success of nonlocal functionals while targeting the computational complexity of GGA functionals. We term the new functional SMP. SMP's "parent" kinetic energy functional features an energy density that is a mix of two functionals

$$\begin{aligned} T_s[\rho] &= \int \tau[\rho](\mathbf{r}) d\mathbf{r} \\ &= \int [W(\rho(\mathbf{r}))\tau_{\text{TF}}(\rho(\mathbf{r})) + (1 - W(\rho(\mathbf{r}))) \\ &\quad \tau_{\text{GGA}}(\rho(\mathbf{r}), s(\mathbf{r}))] d\mathbf{r} \end{aligned} \quad (5)$$

where τ and τ_{GGA} are the total kinetic energy density and the one of a GGA functional, $T_{\text{GGA}}[\rho]$ (we use revAPBEK in this work), respectively. W is a switching function. Mixing functionals is a commonly adopted technique for improving density functionals of either the kinetic energy or the exchange–correlation (xc).^{36–48}

The corresponding kinetic potential is

$$\begin{aligned} v_s[\rho](\mathbf{r}) &= \frac{\delta T_s[\rho]}{\delta \rho(\mathbf{r})} \\ &= W(\rho(\mathbf{r}))v_{\text{TF}}(\rho(\mathbf{r})) + \frac{\partial W(\rho(\mathbf{r}))}{\partial \rho(\mathbf{r})}\tau_{\text{TF}}(\rho(\mathbf{r})) \\ &\quad + [1 - W(\rho(\mathbf{r}))]v_{\text{GGA}}(\rho(\mathbf{r}), s(\mathbf{r})) \\ &\quad - \frac{\partial W(\rho(\mathbf{r}))}{\partial \rho(\mathbf{r})}\tau_{\text{GGA}}(\rho(\mathbf{r}), s(\mathbf{r})) \end{aligned} \quad (6)$$

where $v_{\text{TF}}(\rho(\mathbf{r})) = \frac{\partial \tau_{\text{TF}}(\rho(\mathbf{r}))}{\partial \rho(\mathbf{r})}$ and $v_{\text{GGA}}(\rho(\mathbf{r}), s(\mathbf{r})) = \frac{\partial \tau_{\text{GGA}}(\rho(\mathbf{r}), s(\mathbf{r}))}{\partial \rho(\mathbf{r})} - \nabla \cdot \frac{\partial \tau_{\text{GGA}}(\rho(\mathbf{r}), s(\mathbf{r}))}{\partial \nabla \rho(\mathbf{r})}$. The final kinetic potential can be expressed as

$$\begin{aligned} v_s[\rho](\mathbf{r}) &= v_{\text{GGA}}(\rho(\mathbf{r}), s(\mathbf{r})) + W(\rho(\mathbf{r})) \\ &\quad (v_{\text{TF}}(\rho(\mathbf{r})) - v_{\text{GGA}}(\rho(\mathbf{r}), s(\mathbf{r}))) \\ &\quad + \frac{\partial W(\rho(\mathbf{r}))}{\partial \rho(\mathbf{r})}(\tau_{\text{TF}}(\rho(\mathbf{r})) - \tau_{\text{GGA}}(\rho(\mathbf{r}), s(\mathbf{r}))) \end{aligned} \quad (7)$$

The switching function is defined as a hyperbolic function

$$W(\rho(\mathbf{r})) = \tanh(\rho(\mathbf{r})/\rho^*) = \frac{1 - e^{-2\rho(\mathbf{r})/\rho^*}}{1 + e^{-2\rho(\mathbf{r})/\rho^*}} \quad (8)$$

$$\frac{\partial W(\rho(\mathbf{r}))}{\partial \rho(\mathbf{r})} = \frac{1}{\rho^* \cosh^2(\rho(\mathbf{r})/\rho^*)} \quad (9)$$

where ρ^* is a constant parameter. The $W(\rho(\mathbf{r}))$ function is in the [0–1] range. For the high-density regions ($\rho(\mathbf{r}) > \rho^*$), $W(\rho(\mathbf{r}))$ tends to 1, which means that the TF functional contributes the most. Conversely, for the low-density regions ($\rho(\mathbf{r}) \ll \rho^*$), $W(\rho(\mathbf{r}))$ tends to 0 and the GGA functional contributes the most.

So far, the above equations are appropriate for an approximation for the noninteracting kinetic energy. To obtain a NAKE, we can use the decomposable NAKE formula eq 1. For SMP, the ρ^* parameter is crucial and it is chosen following the steps below:

- 1 Compute the ratio between $\rho_I(\mathbf{r})$ and $\rho(\mathbf{r}) - \rho_I(\mathbf{r})$. Namely

$$S_I(\mathbf{r}) = \frac{\rho_I(\mathbf{r})}{\rho(\mathbf{r}) - \rho_I(\mathbf{r})} \quad (10)$$

- 2 Special points \mathbf{r}_h are those where $S_I(\mathbf{r}_h) = 1$.
- 3 ρ^* is given by the following expression

$$\rho^* = \max_{\mathbf{r}_h} \{\rho_I(\mathbf{r}_h) + \rho(\mathbf{r}_h)\} \quad (11)$$

The parameter ρ^* needs no adjustment during a single-point energy calculation and is unique to each subsystem. The total kinetic energy functional is evaluated with a ρ^* obtained by averaging the ρ^* of all the subsystems. In practice, the special points \mathbf{r}_h are found by the mask condition $0.5 - \text{tol} < \rho_I(\mathbf{r})/\rho(\mathbf{r}) < 0.5 + \text{tol}$, where tol is a tolerance to make sure there are some points that satisfy this condition. Here, we set $\text{tol} = 0.1$. We note that eq 10 is to be evaluated only when the environment density, $\rho(\mathbf{r}) - \rho_I(\mathbf{r})$, is larger than a threshold (1×10^{-6}). When ρ^* is below such a threshold, the parent GGA functional is used.

ρ^* is determined at the beginning of the calculation and kept constant throughout the self-consistent field procedure. This can be potentially problematic during ab-initio molecular dynamics (MD). However, we plan to determine ρ^* from the electron densities of the preceding MD step, avoiding the need to run two single-point calculations (*i.e.*, one for ρ^* and one with SMP employing the determined ρ^*). In this work, for simplicity, we determine ρ^* by performing a preliminary calculation with the revAPBEK NAKE. To dispel doubts about the robustness of the method, we also verified that determining ρ^* self-consistently (*i.e.*, re-running calculations updating ρ^* until

convergence) leads to essentially the same results (see Supporting Information document Figure S1).

We also carried out a stress test to see how sensitive SMP is to the choice of ρ^* . The results in Figure S2 show that while it is important to choose an appropriate ρ^* to recover accurate nonadditive energies, the dependence of SMP to the choice of ρ^* is mild. In practical calculations, the subsystems are spatially separated entities (albeit their densities overlap). Thus, eq 11 applies to a subsystem ($\rho_I(r)$) which only mildly overlaps with the environment ($\rho(r) - \rho_I(r)$). For very strongly overlapping subsystem densities, the sDFT procedure breaks down due to the inaccuracies in the NAKes. Although eq 11 was found by trial and error, we can see from Figure S2 that the ρ^* determined from the equation is very close to the best value which would match exactly the interaction energy against KS-DFT.

Let us analyze eq 11 to make sense of the proposed procedure. First, the special points r_h select regions of space where there is a large overlap between the electron densities of the subsystems. A NAKE should have an awareness of the inter-subsystem density overlap.^{3,35,49,50} Thus, ρ^* depends on the value of the subsystem density at the special points to encode such a dependence. Second, the choice of ρ^* should be such that the switching function in eq 8 correctly weighs the regions of high density (relative to the inter-subsystem overlap), assigning the TF functional to these regions and a GGA functional to the regions of relative low density. We stress that SMP is a NAKE and cannot be used as a KEDF functional.

3. COMPUTATIONAL DETAILS

The molecules are placed in an orthorhombic box, which is large enough so that the nearest-neighbor periodic images are more than 12 Å apart. This ensures that the interactions between the studied systems and their periodic images are negligible. All sDFT calculations in this work were performed with a development version of the in-house eDFTpy Python-based density embedding software,⁵¹ which is based on DFTpy.⁵² All KS-DFT benchmark calculations were performed with the Quantum ESPRESSO (QE) package.⁵³ In both subsystem DFT and KS-DFT calculations, the Perdew–Burke–Ernzerhof (PBE) form of the GGA xc functional is employed.³² The GBRV ultrasoft pseudopotentials⁵⁴ are adopted due to their excellent transferability. The kinetic energy cutoffs of wave function and density are 70 and 400 Ry, respectively. The convergence threshold for self-consistent calculations is 1×10^{-8} Ry.

4. RESULTS AND DISCUSSION

In Table 1, we list MADs of the interaction energies computed with sDFT and various NAKes against the KS-DFT result employing the PBE xc functional. The point of this comparison is to inspect how well the NAKes perform against KS-DFT which employs the exact noninteracting kinetic energy. This is a meaningful comparison^{22,24} because if the NAKE is exact, the KS-DFT result should be recovered. To make sure SMP does not overly rely on error cancellation with the corresponding nonadditive xc functional, we carried out additional calculations for the S22-5 set with sDFT (SMP) and KS-DFT with revPBE as the xc functional. The MAD between the two methods is 0.6 kcal/mol which is identical to the MAD between sDFT (SMP) and KS-DFT when the PBE functional is employed. We conclude that SMP is accurate enough to not display accidental error cancellation when paired to a specific xc functional. A

Table 1. Summary of the MADs of the Interaction Energies Computed with sDFT Carried out with TF, revAPBEK, LMGPA, and SMP NAKes against KS-DFT Results^a

set	functional	hydrogen	dispersion	mixed	total
S22-5	TF	4.40	1.60	1.32	2.40
	revAPBEK	0.82	2.01	0.53	1.16
	LMGPA	0.97	0.89	0.60	0.82
	SMP	0.77	0.88	0.18	0.62
S66	TF	5.08	2.48	2.14	3.28
	revAPBEK	0.58	1.67	0.91	1.06
	LMGPA	1.28	1.24	0.49	1.03
	SMP	0.99	0.38	0.16	0.53

^aAll values are given in kcal/mol.

similar conclusion is reached for nonlocal NAKes, such as LMGPA.^{17,25}

The reader may wonder if the use of pseudopotentials in this work may affect the results. Different pseudopotentials only differ in the pseudo density values at the core region of the atoms and are essentially the same outside of the atomic cores. Thus, we do not expect pseudopotentials to play any significant role besides introducing a slight (expected) variability in the results. To test this assumption, we compute the ρ^* parameter for a formic acid dimer which has the largest inter-subsystem overlap among the systems in the S22 set and therefore is the most vulnerable to be affected by errors introduced by the pseudopotentials. For the test, we chose the GBRV ultrasoft pseudopotentials (US)⁵⁴ and the ONCV norm-conserving pseudopotentials (NC).⁵⁵ The results are $\rho^* = 0.072$ for US and $\rho^* = 0.073$ for NC, confirming our assumption.

As we can see from the table, SMP delivers almost always the most accurate interaction energies for the two data sets chosen (S66 and S22-5) with exception for hydrogen-bonded systems. It is generally known that GGA NAKes like revAPBEK and LC94 are particularly good with hydrogen-bonded systems^{22,56} leading these functionals to describe liquid water very accurately.⁵⁷ The reason for the good behavior of GGA NAKes for hydrogen bonded systems is because the error introduced in the NAKE offsets errors brought in by the nonadditive part of the xc functional^{18,22,58,59} (e.g., the long-range part of the xc functional is known to include errors of self-interaction⁶⁰). SMP, however, is overall of higher quality compared to these GGA functionals and performs even better than a nonlocal functional with density-dependent kernel (LMGPA).^{61,62}

In Figure 1, we break down each contributing dimer to the S22-5 and S66 test sets. From the figure, it is evident why SMP works as a NAKE. SMP effectively interpolates between TF and a GGA functional. GGA functionals, such as revAPBEK, tend to underestimate the binding energy while TF always overestimates the binding energy. An interpolation of the two will naturally improve the binding energy values. However, SMP not only exploits error cancellation to deliver improved binding energies but also does a better job in reproducing the electron densities as we explain below.

The next test is to check the accuracy of the predicted electron density. Once again, we carry out this test against KS-DFT densities. In Table 2, we showcase the density deviations, computed as $\langle \Delta \rho \rangle = 1/2 \int |\rho_{\text{sDFT}}(r) - \rho_{\text{KS-DFT}}(r)| dr$.

The table shows that even though all of the adopted functionals appear to deliver electron densities that are very close to the KS-DFT electron density (all values in the table

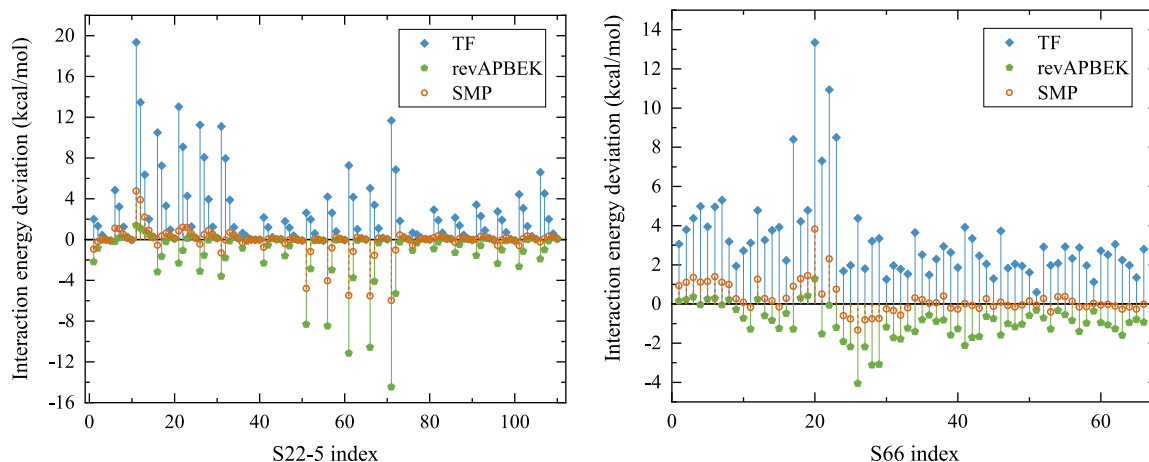


Figure 1. Interaction energy deviations in kcal/mol between sDFT with TF, revAPBEK, and SMP KEDFs against the KS-DFT results for the S22-5 and S66 test sets. Both KS-DFT and sDFT calculations are carried out with the PBE xc functional.

Table 2. MAD of the $\langle\Delta\rho\rangle^a$ Computed with sDFT Carried out with TF, revAPBEK, LMGPA, and SMP NAKEs against KS-DFT Results

set	functional	hydrogen	dispersion	mixed	total
S22-5	TF	3.20	1.40	1.09	1.87
	revAPBEK	3.07	1.67	0.96	1.89
	LMGPA	3.07	1.45	0.90	1.79
	SMP	2.94	1.14	0.87	1.63
S66	TF	3.52	2.08	1.76	2.49
	revAPBEK	3.29	2.17	1.60	2.39
	LMGPA	3.30	1.82	1.47	2.23
	SMP	3.14	1.36	1.32	1.97

^aThe actual values of $\langle\Delta\rho\rangle$ are the values in the table multiplied by 10^{-2} .

should be multiplied by 10^{-2}), SMP outperforms all other functionals. Once again, all functionals, and SMP in particular, do an excellent job with dispersion-bound complexes. However,

they deviate more from the KS-DFT benchmark for hydrogen-bonded complexes.

We conclude this section with an analysis of the performance of the NAKEs considered so far (including SMP) in production-like sDFT simulations by comparing the sDFT interaction energy results against benchmark CCSD(T) values. We choose the PBE + D4 xc functional as it was shown to perform particularly well for weak interactions while maintaining the cost of a semilocal functional.^{63,64} In Figure 2, we show violin plots indicating that for both S22-5 and S66, SMP is the top performer, not only because the MADs are very close to zero ($\text{MAD}_{\text{S22-5}}^{\text{SMP}} = 0.53$ kcal/mol, $\text{MAD}_{\text{S66}}^{\text{SMP}} = 0.68$ kcal/mol) but because the spread of the error is comparable to KS-DFT (for which the D4 corrections were parametrized) and evenly distributed (no bias). The results are comparable with KS-DFT results ($\text{MAD}_{\text{S22-5}}^{\text{KS-DFT}} = 0.33$ kcal/mol, $\text{MAD}_{\text{S66}}^{\text{KS-DFT}} = 0.74$ kcal/mol). Conversely, similar to the results obtained when comparing against KS-DFT, TF and revAPBEK continue to show bias in opposite directions (TF overestimates and

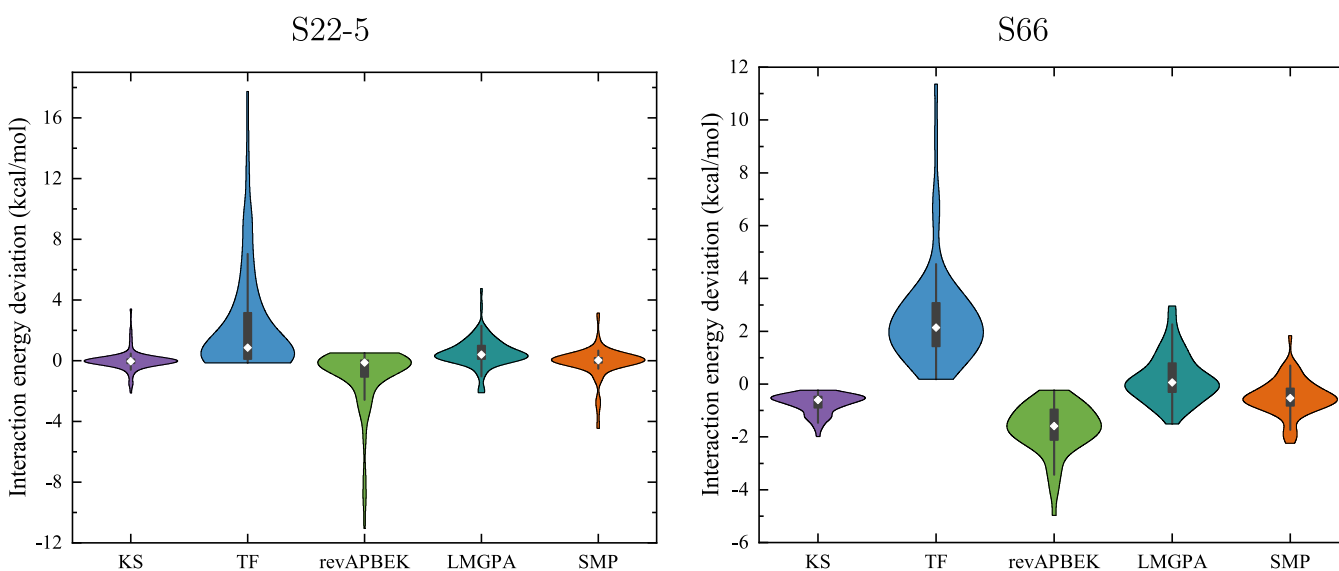


Figure 2. Violin plots overlaid on box plots of the interaction energy deviations of KS-DFT and sDFT with several NAKEs for the S22-5 and S66 test sets comparing against CCSD(T) interaction energies. Both KS-DFT and sDFT are carried out with the PBE + D4 xc functional. The box (thick black bar) in the centre represents the interquartile range and the thin black line indicates the range of data falling within $1.5\times$ box length beyond the upper and lower limits of the box. The white diamond mark in the middle is the median value.

revAPBEK underestimates). The nonlocal LMGPA delivers interaction energy deviations that are slightly more deviated from the benchmark and spread out compared to SMP ($MAD_{S22-5}^{LMGPA} = 0.77$ kcal/mol, $MAD_{S66}^{LMGPA} = 0.69$ kcal/mol).

5. CONCLUSIONS

This work proposes a new nonadditive kinetic energy functional to be used in subsystem DFT (or density embedding) calculations. The developed functional (termed SMP) is inspired by the role of the nonlocal part in nonlocal kinetic energy functionals, that is, to effectively remove the von Weizsäcker functional and only keep Thomas-Fermi in the high-density regions and do the opposite in low-density regions. SMP effectively interpolates from a GGA functional (we choose revAPBEK) to the Thomas-Fermi functional in high-density regions. Additionally, SMP is (sub)system-specific because it contains a parameter, ρ^* , determined automatically and specific to the particular inter-subsystem density overlap occurring in the simulations. SMP is overall very accurate, improving on the two most accurate nonadditive kinetic energy functionals available to date for reproducing conventional DFT and benchmark CCSD(T) interaction energy values for the S22-5 and S66 test sets retaining the computational cost of a semilocal functional.

■ ASSOCIATED CONTENT

Supporting Information

The Supporting Information is available free of charge at <https://pubs.acs.org/doi/10.1021/acs.jctc.1c00283>.

Effect of the parameter ρ^* on the interaction energy (PDF)

■ AUTHOR INFORMATION

Corresponding Authors

Xuecheng Shao – Department of Chemistry, Rutgers University, Newark, New Jersey 07102, United States;
Email: xuecheng.shao@rutgers.edu

Wenhui Mi – Department of Chemistry, Rutgers University, Newark, New Jersey 07102, United States; orcid.org/0000-0002-1612-5292; Email: wenhui.mi@rutgers.edu

Michele Pavanello – Department of Chemistry, Rutgers University, Newark, New Jersey 07102, United States; Department of Physics, Rutgers University, Newark, New Jersey 07102, United States; orcid.org/0000-0001-8294-7481; Email: m.pavanello@rutgers.edu

Complete contact information is available at: <https://pubs.acs.org/doi/10.1021/acs.jctc.1c00283>

Notes

The authors declare no competing financial interest.

■ ACKNOWLEDGMENTS

This material is based upon work supported by the National Science Foundation under grants no. CHE-1553993 and OAC-1931473. We thank the Office of Advanced Research Computing at Rutgers for providing access to the Amarel cluster. Xuecheng Shao acknowledges the Molecular Sciences Software Institute for support through a Software Investment Fellowship.

■ REFERENCES

- (1) Neugebauer, J. *Recent Advances in Orbital-free Density Functional Theory*; Wesolowski, T. A., Wang, Y. A., Eds.; World Scientific: Singapore, 2013.
- (2) Wesolowski, T. A.; Shedge, S.; Zhou, X. Frozen-Density Embedding Strategy for Multilevel Simulations of Electronic Structure. *Chem. Rev.* **2015**, *115*, 5891–5928.
- (3) Jacob, C. R.; Neugebauer, J. Subsystem density-functional theory. *Wiley Interdiscip. Rev.: Comput. Mol. Sci.* **2014**, *4*, 325–362.
- (4) Krishtal, A.; Sinha, D.; Genova, A.; Pavanello, M. Subsystem density-functional theory as an effective tool for modeling ground and excited states, their dynamics and many-body interactions. *J. Phys.: Condens. Matter* **2015**, *27*, 183202.
- (5) Gritsenko, O. V. On the Principal Difference Between the Exact and Approximate Frozen-Density Embedding Theory. *Recent Advances in Orbital-free Density Functional Theory*; Wesolowski, T. A., Wang, Y. A., Eds.; World Scientific: Singapore, 2013; Chapter 12, pp 355–365.
- (6) Wesolowski, T. A. *Computational Chemistry: Reviews of Current Trends*; Leszczynski, J., Ed.; World Scientific: Singapore, 2006; Vol. 10, pp 1–82.
- (7) Senatore, G.; Subbaswamy, K. R. Density Dependence of the Dielectric Constant of Rare-Gas Crystals. *Phys. Rev. B: Condens. Matter Mater. Phys.* **1986**, *34*, 5754–5757.
- (8) Cortona, P. Direct determination of self-consistent total energies and charge densities of solids: A study of the cohesive properties of the alkali halides. *Phys. Rev. B: Condens. Matter Mater. Phys.* **1992**, *46*, 2008–2014.
- (9) Wesolowski, T. A.; Warshel, A. Frozen Density Functional Approach for ab Initio Calculations of Solvated Molecules. *J. Chem. Phys.* **1993**, *97*, 8050.
- (10) Gordon, R. G.; Kim, Y. S. Theory for the Forces between Closed-Shell Atoms and Molecules. *J. Chem. Phys.* **1972**, *56*, 3122.
- (11) Unsleber, J. P.; Neugebauer, J.; Jacob, C. R. No need for external orthogonality in subsystem density-functional theory. *Phys. Chem. Chem. Phys.* **2016**, *18*, 21001–21009.
- (12) Goodpaster, J. D.; Ananth, N.; Manby, F. R.; Miller, T. F., III Exact Nonadditive Kinetic Potentials for Embedded Density Functional Theory. *J. Chem. Phys.* **2010**, *133*, 084103.
- (13) Genova, A.; Ceresoli, D.; Krishtal, A.; Andreussi, O.; DiStasio, R. A., Jr; Pavanello, M. eQE: An open-source density functional embedding theory code for the condensed phase. *Int. J. Quantum Chem.* **2017**, *117*, No. e25401.
- (14) Jacob, C. R.; Neugebauer, J.; Visscher, L. A Flexible Implementation of Frozen-Density Embedding for Use in Multilevel Simulations. *J. Comput. Chem.* **2008**, *29*, 1011–1018.
- (15) Unsleber, J. P.; Dresselhaus, T.; Klahr, K.; Schnieders, D.; Böckers, M.; Barton, D.; Neugebauer, J. Serenity: A subsystem quantum chemistry program. *J. Comput. Chem.* **2018**, *39*, 788–798.
- (16) Höfener, S. The KOALA program: Wavefunction frozen-density embedding. *Int. J. Quantum Chem.* **2020**, *121*, No. e26351.
- (17) Mi, W.; Shao, X.; Genova, A.; Ceresoli, D.; Pavanello, M. eQE 2.0: Subsystem DFT Beyond GGA Functionals. **2021**, arXiv:2103.07556. arXiv preprint.
- (18) Wesolowski, T. A.; Tran, F. Gradient-free and gradient-dependent approximations in the total energy bifunctional for weakly overlapping electron densities. *J. Chem. Phys.* **2003**, *118*, 2072.
- (19) Wesolowski, T. A. Density functional theory with approximate kinetic energy functionals applied to hydrogen bonds. *J. Chem. Phys.* **1997**, *106*, 8516–8526.
- (20) Goez, A.; Neugebauer, J. *Embedding Methods in Quantum Chemistry*. *Frontiers of Quantum Chemistry*; Springer: Singapore, 2017; pp 139–179.
- (21) Fux, S.; Jacob, C. R.; Neugebauer, J.; Visscher, L.; Reiher, M. Accurate frozen-density embedding potentials as a first step towards a subsystem description of covalent bonds. *J. Chem. Phys.* **2010**, *132*, 164101.
- (22) Götz, A. W.; Beyhan, S. M.; Visscher, L. Performance of Kinetic Energy Functionals for Interaction Energies in a Subsystem

Formulation of Density Functional Theory. *J. Chem. Theory Comput.* **2009**, *5*, 3161–3174.

(23) Genova, A.; Ceresoli, D.; Pavanello, M. Periodic Subsystem Density-Functional Theory. *J. Chem. Phys.* **2014**, *141*, 174101.

(24) Schlüns, D.; Klahr, K.; Mück-Lichtenfeld, C.; Visscher, L.; Neugebauer, J. Subsystem-DFT potential-energy curves for weakly interacting systems. *Phys. Chem. Chem. Phys.* **2015**, *17*, 14323–14341.

(25) Mi, W.; Pavanello, M. Nonlocal Subsystem Density Functional Theory. *J. Phys. Chem. Lett.* **2020**, *11*, 272–279.

(26) Kevorkyants, R.; Eshuis, H.; Pavanello, M. FDE-vdW: A van der Waals Inclusive Subsystem Density-Functional Theory. *J. Chem. Phys.* **2014**, *141*, 044127.

(27) Sinha, D.; Pavanello, M. Exact Kinetic Energy Enables Accurate Evaluation of Weak Interactions by the FDE-vdW Method. *J. Chem. Phys.* **2015**, *143*, 084120.

(28) Tran, F.; Wesolowski, T. A. Link between the Kinetic- and Exchange-Energy Functionals in the Generalized Gradient Approximation. *Int. J. Quantum Chem.* **2002**, *89*, 441–446.

(29) Laricchia, S.; Fabiano, E.; Constantin, L. A.; Della Sala, F. Generalized Gradient Approximations of the Noninteracting Kinetic Energy from the Semiclassical Atom Theory: Rationalization of the Accuracy of the Frozen Density Embedding Theory for Nonbonded Interactions. *J. Chem. Theory Comput.* **2011**, *7*, 2439–2451.

(30) Constantin, L. A.; Fabiano, E.; Laricchia, S.; Della Sala, F. Semiclassical neutral atom as a reference system in density functional theory. *Phys. Rev. Lett.* **2011**, *106*, 186406.

(31) Karasiev, V. V.; Trickey, S. B.; Harris, F. E. Born-Oppenheimer Interatomic Forces from Simple, Local Kinetic Energy Density Functionals. *J. Comput.-Aided Mol. Des.* **2006**, *13*, 111–129.

(32) Perdew, J. P.; Burke, K.; Ernzerhof, M. Generalized Gradient Approximation Made Simple. *Phys. Rev. Lett.* **1996**, *77*, 3865–3868.

(33) Huang, C.; Carter, E. A. Nonlocal orbital-free kinetic energy density functional for semiconductors. *Phys. Rev. B: Condens. Matter Mater. Phys.* **2010**, *81*, 045206.

(34) Wang, Y. A.; Carter, E. A. *Theoretical Methods in Condensed Phase Chemistry*; Schwartz, S. D., Ed.; Kluwer: Dordrecht, 2000; pp 117–184.

(35) Jiang, K.; Nafziger, J.; Wasserman, A. Constructing a non-additive non-interacting kinetic energy functional approximation for covalent bonds from exact conditions. *J. Chem. Phys.* **2018**, *149*, 164112.

(36) Ghassemi, E. N.; Somers, M. F.; Kroes, G.-J. Assessment of Two Problems of Specific Reaction Parameter Density Functional Theory: Sticking and Diffraction of H₂ on Pt(111). *J. Phys. Chem. C* **2019**, *123*, 10406–10418.

(37) Tchakoua, T.; Smeets, E. W. F.; Somers, M.; Kroes, G.-J. Toward a Specific Reaction Parameter Density Functional for H₂ + Ni(111): Comparison of Theory with Molecular Beam Sticking Experiments. *J. Phys. Chem. C* **2019**, *123*, 20420–20433.

(38) Smeets, E. W. F.; Voss, J.; Kroes, G.-J. Specific Reaction Parameter Density Functional Based on the Meta-Generalized Gradient Approximation: Application to H₂ + Cu(111) and H₂ + Ag(111). *J. Phys. Chem. A* **2019**, *123*, 5395–5406.

(39) Peng, H.; Yang, Z.-H.; Perdew, J. P.; Sun, J. Versatile van der Waals Density Functional Based on a Meta-Generalized Gradient Approximation. *Phys. Rev. X* **2016**, *6*, 041005.

(40) Mardirossian, N.; Head-Gordon, M. Mapping the genome of meta-generalized gradient approximation density functionals: The search for B97M-V. *J. Chem. Phys.* **2015**, *142*, 074111.

(41) de Silva, P.; Corminboeuf, C. Communication: A new class of non-empirical explicit density functionals on the third rung of Jacob's ladder. *J. Chem. Phys.* **2015**, *143*, 111105.

(42) De Silva, P.; Corminboeuf, C. Local hybrid functionals with orbital-free mixing functionals and balanced elimination of self-interaction error. *J. Chem. Phys.* **2015**, *142*, 074112.

(43) Schmidt, T.; Kraissler, E.; Makmal, A.; Kronik, L.; Kümmel, S. A self-interaction-free local hybrid functional: Accurate binding energies vis-à-vis accurate ionization potentials from Kohn-Sham eigenvalues. *J. Chem. Phys.* **2014**, *140*, 18A510.

(44) Maier, T. M.; Arbuznikov, A. V.; Kaupp, M. Local hybrid functionals: Theory, implementation, and performance of an emerging new tool in quantum chemistry and beyond. *Wiley Interdiscip. Rev.: Comput. Mol. Sci.* **2019**, *9*, No. e1378.

(45) Jaramillo, J.; Scuseria, G. E.; Ernzerhof, M. Local hybrid functionals. *J. Chem. Phys.* **2003**, *118*, 1068–1073.

(46) Mejia-Rodriguez, D.; Trickey, S. B. Deorbitalization strategies for meta-generalized-gradient-approximation exchange-correlation functionals. *Phys. Rev. A* **2017**, *96*, 052512.

(47) Sun, J.; Ruzsinszky, A.; Perdew, J. P. Strongly Constrained and Appropriately Normed Semilocal Density Functional. *Phys. Rev. Lett.* **2015**, *115*, 036402.

(48) Perdew, J. P.; Constantin, L. A. Laplacian-level density functionals for the kinetic energy density and exchange-correlation energy. *Phys. Rev. B: Condens. Matter Mater. Phys.* **2007**, *75*, 155109.

(49) Lastra, J. M. G.; Kaminski, J. W.; Wesolowski, T. A. Orbital-free effective embedding potential at nuclear cusps. *J. Chem. Phys.* **2008**, *129*, 074107.

(50) Jacob, C.; Visscher, L. *Recent Progress in Orbital-free Density Functional Theory*; Wesolowski, T. A., Wang, Y. A., Eds.; World Scientific: Singapore, 2013; pp 299–324.

(51) Shao, X.; Mi, W.; Pavanello, M. eDFTpy: An object-oriented platform for density embedding simulations. **2021** in preparation; edftpy.rutgers.edu

(52) Shao, X.; Jiang, K.; Mi, W.; Genova, A.; Pavanello, M. DFTpy: An efficient and object-oriented platform for orbital-free DFT simulations. *Wiley Interdiscip. Rev.: Comput. Mol. Sci.* **2021**, *11*, No. e1482.

(53) Giannozzi, P.; Andreussi, O.; Brumme, T.; Bunau, O.; Buongiorno Nardelli, M.; Calandra, M.; Car, R.; Cavazzoni, C.; Ceresoli, D.; Cococcioni, M.; Colonna, N.; Carnimeo, I.; Dal Corso, A.; de Gironcoli, S.; Delugas, P.; DiStasio, R. A.; Ferretti, A.; Floris, A.; Fratesi, G.; Fugallo, G.; Gebauer, R.; Gerstmann, U.; Giustino, F.; Gorni, T.; Jia, J.; Kawamura, M.; Ko, H.-Y.; Kokalj, A.; Küçükbenli, E.; Lazzeri, M.; Marsili, M.; Marzari, N.; Mauri, F.; Nguyen, N. L.; Nguyen, H.-V.; Otero-de-la-Roza, A.; Paulatto, L.; Poncè, S.; Rocca, D.; Sabatini, R.; Santra, B.; Schlipf, M.; Seitsonen, A. P.; Smogunov, A.; Timrov, I.; Thonhauser, T.; Umari, P.; Vast, N.; Wu, X.; Baroni, S. Advanced capabilities for materials modelling with Quantum ESPRESSO. *J. Phys.: Condens. Matter* **2017**, *29*, 465901.

(54) Garrity, K. F.; Bennett, J. W.; Rabe, K. M.; Vanderbilt, D. Pseudopotentials for high-throughput DFT calculations. *Comput. Mater. Sci.* **2014**, *81*, 446–452.

(55) Hamann, D. R. Optimized norm-conserving Vanderbilt pseudopotentials. *Phys. Rev. B: Condens. Matter Mater. Phys.* **2013**, *88*, 085117.

(56) Kevorkyants, R.; Dulak, M.; Wesolowski, T. A. Interaction energies in hydrogen-bonded systems: A testing ground for subsystem formulation of density-functional theory. *J. Chem. Phys.* **2006**, *124*, 024104.

(57) Genova, A.; Ceresoli, D.; Pavanello, M. Avoiding Fractional Electrons in Subsystem DFT Based Ab-Initio Molecular Dynamics Yields Accurate Models For Liquid Water and Solvated OH Radical. *J. Chem. Phys.* **2016**, *144*, 234105.

(58) Wesolowski, T. A.; Morgantini, P.-Y.; Weber, J. Intermolecular interaction energies from the total energy bifunctional: A case study of carbazole complexes. *J. Chem. Phys.* **2002**, *116*, 6411–6421.

(59) Tran, F.; Weber, J.; Wesolowski, T. A. Theoretical Study of the Benzene Dimer by the Density-Functional-Theory Formalism Based on Electron-Density Partitioning. *Helv. Chim. Acta* **2001**, *84*, 1489–1503.

(60) Ruzsinszky, A.; Perdew, J. P.; Csonka, G. I.; Vydrov, O. A.; Scuseria, G. E. Spurious fractional charge on dissociated atoms: Pervasive and resilient self-interaction error of common density functionals. *J. Chem. Phys.* **2006**, *125*, 194112.

(61) Mi, W.; Genova, A.; Pavanello, M. Nonlocal kinetic energy functionals by functional integration. *J. Chem. Phys.* **2018**, *148*, 184107.

(62) Mi, W.; Pavanello, M. Orbital-Free DFT Correctly Models Quantum Dots When Asymptotics, Nonlocality and Nonhomogeneity Are Accounted For. *Phys. Rev. B* **2019**, *100*, 041105.

(63) Caldeweyher, E.; Bannwarth, C.; Grimme, S. Extension of the D3 dispersion coefficient model. *J. Chem. Phys.* **2017**, *147*, 034112.

(64) Caldeweyher, E.; Ehlert, S.; Hansen, A.; Neugebauer, H.; Spicher, S.; Bannwarth, C.; Grimme, S. A generally applicable atomic-charge dependent London dispersion correction. *J. Chem. Phys.* **2019**, *150*, 154122.